EIGHTH EUROPEAN ROTORCRAFT AND POWERED LIFT AIRCRAFT FORUM

Paper No. 2.8

ADVANCED ROTOR ANALYSIS METHODS FOR THE AERODYNAMICS OF VORTEX/BLADE INTERACTIONS IN HOVER

J. Michael Summa

Analytical Methods, Inc.
P.O. Box 3786
Bellevue, Washington 98009
U.S.A.

August 31 - September 3, 1982

Aix-en-Provence,
France

Abstract

The work discussed in this report has shown that the complete hovering rotor wake geometry, including the inner sheet, can be predicted without the constraints or empiricisms of a prescribed wake. Moreover, the calculated wakes for some modern rotors violate the usual hypothesis in prescribed wake methods of a weak linear inner sheet and a single rolled-up tip vortex. When coupled with a lifting-surface method, this relaxed wake procedure allows for the accurate analysis of rotor performance at proper collective settings. Finally, the application of a surface singularity method developed for rotors has demonstrated the capability of accurately computing blade surface pressures very near the rotor tip edge.

1.0 INTRODUCTION

In the last twenty-five years, a great deal of progress has been made in the design of the helicopter. Rotary wing aircraft are now faster, more efficient, quieter and carry more payload than ever before. These advances are a direct result of improved understanding of helicopter aerodynamics that has come with the development of better analytical methods and experimental techniques; however, the latest technology rotor designs that strive for more performance improvement through various combinations of large twist (possibly nonlinear), tapered or swept planforms, and modern airfoils with reflexed camber are beyond the modelling capabilities of most aerodynamic analysis methods in current use. Shortcomings of earlier methods include not only the simple representation of the blade geometries but, more importantly, the coupling of the resultant wake structure with the computed blade loading. These vortex/surface interactions continue to be the most challenging problem in the realistic performance prediction of rotor airloads in hover and in forward flight. Of course, the rotary wing aircraft in forward flight is fraught with other difficult and challenging aerodynamic problems--unsteady separations, highly three-dimensional flows, body-rotor interference and unsteady transonic flows. Still, as far as isolated rotor performance is concerned, the proper modelling of the various wake-blade interactions (this includes the coupled effect of the blade on the vortex core as well as the traditionally recognized effect of the vortex on the blade) holds the greatest promise of more accurate analysis.

In this paper, the application of two analysis methods, a lifting-surface and a surface-singularity method, that are under continued development at Analytical Methods, Inc. for the prediction of hover/climb airloads associated with these new rotors is discussed. The preliminary development of AMI's lifting-surface program, HOVER, was described at the Fifth European Rotorcraft and Powered Lift Aircraft Form in 1979.[1] In this preliminary work, wakes were relaxed in the axial direction only while the radial coordinates were constrained to the prescribed wake locations in order to control numerical instabilities in the calculation of wake position. Since that time, this method has matured into a production program with new techniques for representing the vortex roll-up and computing the complete free-wake coupling as well as the effects of structural elasticity. The free-wake method is described below along with example calculations that illustrate the computational accuracy of the method and its ability to model wakes associated with "unusual" radial circulation distributions.

Finally, a Green's function surface-singularity method that has been developed to examine the detailed pressure distributions of rotor blades of arbitrary shape is discussed. This new program, ROTAIR, includes the effects of the thick blade surface and is therefore the first step toward the eventual goal of the elimination of the two-dimensional constraints in the profile power predictions. The calculated pressure distribution very near the tip of a low aspect ratio blade is compared below with experimental data. The favorable comparison of the suction pressures under the tip vortex formed at the tip illustrates the capability of the method to calculate close vortex interference.

2.0 LIFTING-SURFACE METHOD (PROGRAM "HOVER")

2.1 Blade Representation and Computation Procedure

A "linearized" lifting-surface representation of the rotor airloads is accomplished by a vortex lattice placed on the rotor planform area in the disk plane as illustrated in Figure 1. The distribution of panels is controlled by the user with an option available to automatically generate panels in the manner described by Lan,[2] which allows for a more accurate calculation of leading-edge suction. In HOVER, the influences of individual panels in the blade lattice are computed by quadrilateral vortex rings; therefore, the basic unknowns in the flow tangency equations are the panel ring vortex strengths, or, equivalently, panel doublet strengths. The program includes prescribed as well as relaxed wake calculations. If the user has supplied elastic blade properties, the elastic twist and bending deformations and their impact on the rotor loads are computed during the program iterations. The user can also request a thrust coefficient and the program will adjust the collective setting through the prescribed wake iteration to obtain the required thrust. The relaxed wake calculation then proceeds at fixed collective.

Once a converged wake geometry is computed by the prescribed wake or relaxed wake options, inviscid forces and moments on the blade bound vortex segments are then evaluated in the usual way by applying the Kutta-Joukowski Law. Of course, the chordwise and radial pressure jump distributions are also calculated, and the influence of compressibility is included in the manner described by Sopher.[3]

Finally, with the sectional coefficient of lift distribution known from the lifting-surface calculation, the profile drag and, hence, profile and total torque must be determined by falling back on empirical data. This reliance on empiricism can only be removed when a full thickness model such as that described in Section 4 is used in conjunction with a rigorous viscous flow analysis.

2.2 Wake Modelling

The discrete vortex filaments shed from the trailing edge of each blade represent the hovering rotor wake, which quickly separates into two parts for conventional rotors--an inboard sheet of weaker vorticity and an outer tip sheet that rapidly rolls up to form a very strong tip vortex.[4] It will be shown in the next section that this traditional concept of the rotor wake does not apply for some modern configurations. Details of the prescribed wake representation and the wake segmentation used in HOVER can be found in Reference 1. Options for generating the prescribed wake coordinates include the Kocurek/Tangler wake[5] and the Landgrebe wake.[6] The equations are unchanged except for the description of the vortex springing from the rotor tip edge. A simple model included in HOVER, and shown in Figure 1, of this tip vortex shedding across the blade chord improves the prediction of aerodynamic loading near the rotor tip.

The overall wake structure in the HOVER program is illustrated in Figure 2 and consists of near-, intermediate- and far-wake regions. The dimensionless axial coordinates at the start of the intermediate- and far-wake regions are ZFAR1 and ZFAR2, respectively. The near-wake region generally includes four vortex passes below the generating blade and is the region of wake relaxation. The intermediate-wake region serves as a "buffer" zone between the near-wake filaments and far-wake model. In the far-wake, each helical vortex filament is continued as a semi-infinite cylindrical sheath of uniform vorticity. The far-wake velocity contribution is then computed by the equivalent source disc located at ZFAR2. The addition of this analytical far-wake model is required to eliminate wake length as a parameter in the performance predictions. Figure 3 illustrates the dependency of rotor performance on wake length for an example two-bladed rotor. The calculations show that if the wake is merely truncated, at ZFAR2 = 1.5 (or 6 revolutions) the thrust and figure of mertit are still overpredicted, approximately 4% and 5%, respectively. Of course, the calculation is even more inaccurate for shorter wake lengths. In contrast, the detailed wake can be shortened with no loss in accuracy to a length less than ZFAR2 = 0.5 (2.5 revolutions) if the far-wake model is included with no loss in accuracy.

Generally, the calculated thrust at the completion of the prescribed wake iteration for fixed blade collective is too high and a relaxed wake iteration is required to compute realistic rotor performance. This is because the empirical equations are derived from experimental data of thrust, torque, and tip-vortex filament geometry. Consequently, prescribed wake programs demonstrate good correlation for integrated loads for a large number of conventional rotors since the prescribed wake constants are intimately related to the theoretical methods used to construct the empiricisms. However, these methods are less successful when compared with known collective settings,[7] which implies that although integrated performance is predicted properly, local sectional loads may not be properly calculated. Certainly, if the wake itself deviates from the experimental data base for the prescribed wake constants, performance predictions could be significantly in error.

The method for obtaining relaxed or force-free wake geometries has been modified since it was reported in Reference 1 in order to obtain the radial contraction deformations as well as the axial deformations of rotor wakes. The Scully core model[8] is still used in the program and self-induced velocities continue to be calculated by an expression[1] derived from the procedure reported by Widnall.[9] Briefly, new features of the relaxation procedure are the following.

(1) Grid-Plane Relaxation--

The procedure for obtaining a new wake geometry from calculated wake velocities has been simplified. Basically, velocity components along vortex filaments are computed in cylindrical polar coordinates. The radial, V_R, and axial, V_Z, velocity components are integrated over a time step that is adjusted by the average tangential, V_T , velocity components across the particular wake segment. Consequently, the final wake azimuthal gridding remains fixed throughout the relaxation iterations, and wake deformations are computed in these azimuthal planes.

For rotors with conventional radial circulation distributions, this method converges quite rapidly. More troublesome rotors that are out of the prescribed wake data base and that have circulation distributions exhibiting two or more maxima have required an alternating procedure where axial and radial deformations are calculated on different relaxation iterations. Example calculations are described in Section 3.

(2) Tip Vortex Strength/Wake Regeneration--

The calculated radial circulation distribution is analysed at each prescribed or relaxed wake iteration to calculate the inboard extent of the tip vortex roll-up. During the relaxed wake iterations, if the radial position of the maximum circulation shed into the tip vortex changes by more than 4% of the radius, then the wake segmentation is regenerated, growing or eliminating the necessary "inner sheet" filaments, based on prescribed wake constants computed from the current relaxed wake position.

(3) Relaxation Simplifications--

The HOVER code includes the option of computing the tip vortex deformation by the relaxation method and prescribing an associated inner sheet geometry based upon the current tip vortex position. This is usually sufficient for conventional rotors. A number of other techniques have also been investigated to reduce computation. Relaxation of just two inner sheet filaments and extrapolating inbetween for the remaining ones, or characterization of the wake velocity variation with azimuth by simple functions and computing velocities at a reduced number of node pointscan also be effective. For example, the axial velocity components along the tip vortex can be correctly simplified as a linear function of azimuth up to first blade passage. This implies, by the way, that the prescribed tip vortex axial displacement equations should contain a second-order term in ψ. Once more, however, the coupled behavior of the inner sheet and tip vortex can also violate these "a priori" assumptions. For this reason, the full wake relaxation option is retained in the HOVER code as well.

Finally, a continuing limitation of the relaxed wake method is the prescribed merger of the outer sheet into the tip vortex at an azimuth position, ψ_{MERGER}, set by the user. The calculation of the details of the roll-up process is presently being studied at AMI and will eventually be included in the program.

3.0 RELAXED WAKE/HOVER PERFORMANCE CALCULATIONS

3.1 Correlations for a Conventional Blade

Experimental data of wake geometry and integrated performance for an untwisted, rectangular planform, two-bladed model rotor of aspect ratio 13.7 was reported in Reference 10. The measured wake geometry data was reported to be in agreement with the prescribed wake equations of References 5 and 6. Hence, the calculated wake geometry should remain relatively fixed during the relaxation iterations. For these calculations, the full wake was relaxed and calculations were initiated with Landgrebe's[5] and Kocurek's[6] prescribed wake geometry. The computed collective was adjusted to obtain a thrust coefficient equal to that measured in the test. The computed wake geometry converged to a unique position regardless of the starting geometry.

Figure 4 compares the measured and calculated tip vortex geometry for five relaxed wake iterations for $C_T = 0.0037$. The calculated geometry is well within the scatter of the experimental data,[11] and there is very little movement of the tip vortex through the relaxation iteration. Figure 5 illustrates several constant azimuthal cuts through the inner sheet and tip vortex for the last relaxed wake iteration. For $\psi = 90^o$ and 180^o there are no plottable differences in these geometries when compared with the second relaxation iteration. Moreover, the inner sheet does remain linear as expected with only a slight roll-up indicated at the outboard end where the vorticity is extremely weak.

The measured trend of trust coefficient, C_T, with collective, θ_{75}, and torque coefficient, C_Q, is also predicted quite well as shown in Table 1.

MEASURED			PREDICTED		
θ_{75}*	C_T	$C_Q \times 10^3$	θ_{75}	C_T	$C_Q \times 10^3$
5 ± ½°	.0018	.109	5.2°	.0018	.117
8 ± ½°	.0037	.253	8.5°	.0037	.250
12 ± ½°	.0056	.493	12.1°	.0056	.439

* Reference 11

Table 1. Detailed Comparison of Measured and Calculated Hover Performance for the Ames Untwisted Rotor.

The difference in the C_Q for the 12^o is probably due to separations that occur at the lower test Reynolds number. The corresponding performance map comparison is shown in Figure 6 where the usual ± 2% experimental error band on C_T for fixed C_Q has been applied. These results (and others not reported here) confirm that, for classical rotor blades, the HOVER program accurately predicts performance and wake geometry at the proper collective.

3.2 Correlations for a Highly Twisted and Tapered Blade

HOVER performance calculations for a variety of modern rotor planform geometries have generally compared quite favorably with available experimental data. A rotor of current interest that also represents a real challenge for deformed wake rotor analysis methods is that suggested by Bingham.[12] This two-bladed rotor is linearly tapered (taper ratio = 3:1) from the 50% radius station to the rotor tip. The blade includes three modern reflexed camber airfoil geometries of decreasing thickness across the radius, and incorporates a linear twist rate, θ_1, of -14.0^o. This geometry effectively shifts the thrust loading from the tip to the inboard part of the blade. The resulting wake geometry is completely out of the prescribed wake data base. In fact, the relaxed wake calculations indicate that the prescribed wake equations do a poor job of representing the wake from this rotor.

Kocurek's formulas[6] were specified in the prescribed wake cycle for this rotor. The calculated radial distribution of circulation for the Bingham rotor at a collective setting, θ_{75}, equal to 8.8^o is shown in Figure 7. Here, the prescribed wake circulation distribution is compared with that calculated at the final relaxed wake iteration. The load distribution changes dramatically through the relaxation cycle as the tip vortex moves closer to the blade, and the integrated thrust coefficient decreases by more than 10% as indicated in the figure. The predicted shed wake is composed of an inner sheet of negative and positive vorticity (passing through zero at about the 60% radial station), a secondary rolled-up vortex equal to about 25% of the tip vortex strength (but of opposite direction) shed from the 90% radial station and, lastly, the conventional tip vortex shed from the outer 8% of the blade.

The calculated geometry of the wake is in marked contrast to those of the prescribed wake data base. The presence of the secondary vortex affects not only the tip vortex position, but also results in a "bucket" shaped inner sheet geometry as shown in Figure 8, which illustrates wake cross-sections for the last wake iteration. The relaxation of this wake required alternating calculated axial and radial deformations in order to obtain converged, numerically stable wake geometries.

The axial and radial tip vortex coordinates form the last five relaxation iterations are presented in Figures 9(a) and 9(b), respectively. The earlier iterations are lost in the graphics program because a wake generation was required during the relaxation cycle just before these last five iterations (see Section 2.2). The tip vortex has obviously assumed a stable, force-free position. Similar graphical displays of the inner sheet filaments also reveal a converged wake solution. The relaxed position is compared in these figures with the prescribed wake geometries suggested by Landgrebe[5] (based on the final relaxed wake thrust coefficient) and that suggested by Kocurek[13] for circulation coupling (based on the final relaxed wake tip vortex strength). The radial contraction appears to be adequately modelled in both prescribed wake methods; however, the prescriptions for the tip vortex axial location is poorly represented.

Finally, the computed relaxed wake integrated performance is compared with the experimental data in Figure 10. The calculated performance is shown as a hatched area. At the higher thrusts, this hatched area corresponds to the small changes in thrust that occur during the last five relaxations; however, the hatched area is increased at the lower thrust settings because the relaxed wake iteration indicates a possible vortex impact with the following blade. During the relaxation at low thrust, the tip vortex would cycle from just above to just below the following blade ($Z_W \sim \pm 0.001$) and the computed performance would oscillate within the band indicated in Figure 10. With the exception of the lowest thrust, the calculations are all within ± 2% of the experimental data.

4.0 SURFACE-SINGULARITY METHOD (PROGRAM "ROTAIR")

The surface-singularity method for predicting blade surface pressures in hover or climb is described in detail in Reference 13. The basic methodology for this method was developed for fixed-wing applications involving unsteady oscillations.[14] Rotary wing wake technology has been added to the basic method along with the necessary methods to calculate rotorcraft airloads. The resulting computer code, named ROTAIR, is, therefore, based on technologies developed in HOVER and the fixed-wing computer programs. The actual blade surface including thickness, twist, coning, and the tip-edge closure is represented by finite panels of unknown doublet strength for the surface potential. The integral equation for the velocity potential is derived from Green's theorem, and the internal Dirichlet boundary condition of zero perturbation potential inside the closed body or blade is enforced to obtain the required potential doublet distribution on the blade surface. The effects of the onset flow, including blade rotation, are represented in the solution by the source potential distribution on the blade surface that is required by the Neumann flow tangency condition. This method of solving for the velocity potential on the blade surface offers several numerical advantages since it is one order less singular than the velocity induced by a potential doublet distribution. For example, in Reference 15 it was demonstrated that for comparable density of control points where the boundary conditions are satisfied, the low-order method gives comparable accuracy to the higher-order solutions. It was also shown that problems associated with some earlier low-order panel methods, e.g., leakage in internal flows and junctions and also poor trailing-edge solutions, do not appear for the velocity potential method.

Once the surface potential distribution is known, the surface gradient of the potential is evaluated from a two-way second-order interpolation through the doublet values to obtain the surface velocities. The surface pressure distribution is then computed in the usual manner with compressibility effects included in the same way as in the HOVER code. Resulting inviscid airloads are calculated by surface integration and profile losses are obtained by interpolation in user supplied profile drag tables.

The wake modelling in ROTAIR is essentially carried over from program HOVER with certain required modifications. For example, the velocity potential induced by the far-wake is that due to the superposition of cylindrical potential sheaths of linearly increasing doublet distribution. Also, the tip separation wake is modelled as illustrated in Figure 11. The user specifies the chordwise extent of the separation; the height above the trailing edge that the tip vortex attains, DELZ; and the inboard shift of the tip vortex across the blade surface at the trailing edge, DELR. As a first approximation, DELZ and DELR can be set to a distance corresponding to the tip vortex leaving the blade surface at 1/2 the tip section geometric angle of attack. As experience is gained with the tip shedding, this procedure will be automated within the code. For this model, the feeding sheet filament effects are included, and the actual wake panelling of separated wake is automatically generated.

Although relaxed wake procedure is also included in ROTAIR, the program is usually run with a prescribed wake whose vortex coordinates are obtained from the relaxed wake geometry predicted by HOVER for the same configuration.

Preliminary calculations have verified the capabilities of the program for computing blade surface properties in the presence of a close-vortex passage. Additionally, calculated pressure distributions compare favorably with experimental data for a low aspect ratio two-bladed rotor, and the calculated circulation distribution is comparable with that computed by the lifting-surface code.[13] Here, calculations with ROTAIR are illustrated by the comparison of the calculated pressure distribution with experimental data very near the tip of a low aspect ratio blade.

5.0 SURFACE PRESSURE COMPARISONS

Detailed chordwise pressure distributions for a single-bladed rectangular rotor of aspect ratio 3 have been measured by Gray et al.[16] Data was collected for flat tip and rounded tip edges. Calculations are compared here for the flat tip rotor. For this low aspect ratio, modelling of the tip vortex shedding across the blade tip chord is a necessity for prediction of rotor loads. This is demonstrated in Figure 12 where the radial distribution of thrust loading computed by HOVER is compared for the tip vortex shedding model switched on and off. A relatively large increase in the normal loads due to the tip vortex shedding is shown for the last 20% of the blade radius. The thrust and induced torque are increased by approximately 5% and 6%, respectively. Basically, the radial extent of the effects of the tip vortex shedding is on the order of 1.5 to 2.0 blade chords.

Chordwise surface pressure distributions compare favorably with the experimental data at all inboard stations. Figure 13 ilustrates the data correlation at the 98.7%, 99.1% and 99.5%

radial locations. The calculated suction pressures under the vortex formed at the tip are accurately predicted for all but the last station at the 99.5% radius. For these calculations, the location of the tip vortex at the blade trailing edge and the chordwise extent of vortex separation were estimated from the experimental data. The calculations are for DELR = 0.015, DELZ = 0.01, and a separation at 38% of the chord from the leading edge (see Figure 11). The calculated suction pressures below the vortex are admittedly very sensitive to DELR (DELZ corresponds very closely to the low aspect ratio theory result). Research is currently being pursued at AMI to calculate the details of the vortex roll-up and the extent of the chordwise separation near wing tips. Until this is possible, this dependency on the prescribed geometry of the tip vortex sheet is unavoidable. Still, these comparisons illustrate the capability of the method to accurately calculate rotary wing surface pressures for difficult problems such as close vortex interferences.

6.0 CONCLUSIONS AND RECOMMENDATIONS

The work discussed in this report has shown that the complete hovering rotor wake geometry, including the inner sheet, can be predicted without the constraints or empiricisms of a prescribed wake. Example calculations presented in the paper demonstrate stable, free-wake geometries for both a traditional and an unconventional rotor blade. This has been achieved through refinements in the basic wake model and in the numerical relaxation procedure. It is shown that the wake structure for some modern rotors does not trend with current prescribed wake empirical equations. The effects of a secondary rolled-up vortex generated near the tip vortex and stronger shed positive and negative vorticity inboard produce a wake geometry that violates the usual hypothesis of a weak linear inner sheet and a single tip vortex. When coupled with a lifting-surface method, this relaxed wake scheme allows for the accurate analysis of rotor performance at proper collective settings.

The application of a surface singularity method for the prediction of detailed surface pressures on rotor blades in hover or climb has also been discussed. Preliminary calculations and comparisons with experiment have verified the capabilities of the method for computing blade surface properties very near the tip edge in the presence of the shed tip vortex.

Further analytical work should include the calculation of the detailed roll-up process in order to eliminate the currently required prescribed merger point. The calculation of the extent of tip-edge vortex separation should also be investigated along with the removal of the present two-dimensional assumptions in the profile power calculation by adding a proper boundary layer calculation scheme to the existing surface singularity method. Finally, it is hoped that future experimental programs will provide the foundation data to verify and develop these techniques for rotor aerodynamic analysis and lead the way to improve rotor designs.

ACKNOWLEDGEMENTS

The author gratefully acknowledges the many helpful conversations regarding this work with his colleagues at AMI and the support given by the U.S. Army Research and Technology Laboratories (AVRADCOM), Ft. Eustis, VA (Contract DAAK51-81-C-0006), and by the U.S. Army Research Office, Research Triangle Park, N.C. (Contract DAAG29-81-C-0032).

REFERENCES

1. Summa, J.M. and Maskew, B., "New Methods for the Calculation of Hover Airloads", Fifth European Rotorcraft and Powered Lift Aircraft Forum, Paper No. 15, Amsterdam, The Netherlands, September 1979.

2. Lan, C.E., "A Quasi Vortex-Lattice Method in Thin Wing Theory", J. Aircraft, Vol. 11, No. 9, September 1974.

3. Sopher, R., "Three-Dimensional Potential Flow Past the Surface of a Rotor Blade", Presented at the 24th Annual National Forum of the American Helicopter Society, Washington, D.C., May 1979.

4. Gray. R.B., "On the Motion of the Helical Vortex Shed from a Single-Bladed Hovering Helicopter Rotor and its Application to the Calculation of the Spanwise Aerodynamic Loading, Princeton Univerity Aeronautical Engineering Department, Report No. 313, September 1955.

5. Landgrebe, A.J., "An Analytical and Experimetnal Investigation of a Helicopter Rotor Hover Performance and Wake Geometry Characteristics", USAAMRDL Technical Report No. 71-24, Eustis Directorate, U.S. Army Air Mobility Research and Development Laboratory, Ft. Eustis, VA, June 1971.

6. Kocurek, J.D. and Tangler, J.L., "Prescribed Wake Lifting Surface Hover Performance Analysis", Presented at the 32nd Annual National VSTOL Forum of the American Helicopter Society, Washington, D.C., May 1976.

7. Caradonna, F.X. and Tung, C., "Experimental and Analytical Studies of a Model Helicopter Rotor in Hover", Sixth European Rotorcraft and Powered Lift Aircraft Forum, Paper No. 25, Bristol, England, September 1980.

8. Scully, M.B., "Computation of Helicopter Rotor Wake Geometry and its Influence on Rotor Harmonic Airloads", MIT ASRL-TR-178-1, March 1971.

9. Widnall, S.E., "The Structure and Dynamics of Vortex Filaments", Annual Review of Fluid Mechanics, Vol. 7, 1975.

10. Tung, C. et al., "The Structure of Trailing Vortices Generated by Model Rotor Blades", Seventh European Rotorcraft and Powered Lift Aircraft Forum, Paper No. 4, Garmisch-Partenkirchen, FRG, September 1981.

11. Tung, C., NASA Ames, Private Communication, 1982.

12. Bingham, G., "The Aerodynamic Influences of Rotor Blade Airfoils, Twist, Taper and Solidity on Hover and Forward Flight Performance", Presented at the 37th Annual Forum of the American Helicopter Society, New Orleans, LA, May 1981.

13. Kocurek, D. et al., "Hover Performance Methodology at Bell Helicopter Textron", Presented at the 36th Annual Forum of the American Helicopter Society, Washington, D.C., May 1980.

14. Summa, J.M. and Maskew, B., "A Surface Singularity Method for Rotors in Hover or Climb", USAAVRADCOM-TR-81-D-23, December 1981.

15. Maskew, B., "Influence of Rotor Blade Tip Shape on Tip Vortex Shedding--An Unsteady, Inviscid Analysis", Presented at the 36th Annual Forum of the American Helicopter Society, Preprint No. 80-6, May 1980.

16. Maskew, B., "Prediction of Subsonic Aerodynamic Characteristics--A Case for Low-Order Panel Methods", AIAA 19th Aerospace Sciences Meeting, AIAA-81-0252, January 1981.

17. Gray, R.B., McMahon, H.M., Shenoy, K.R. and Hammer, M.L., "Surface Pressure Measurements at Two Tips of a Model Helicopter Rotor in Hover", NASA CR-3281, May 1980.

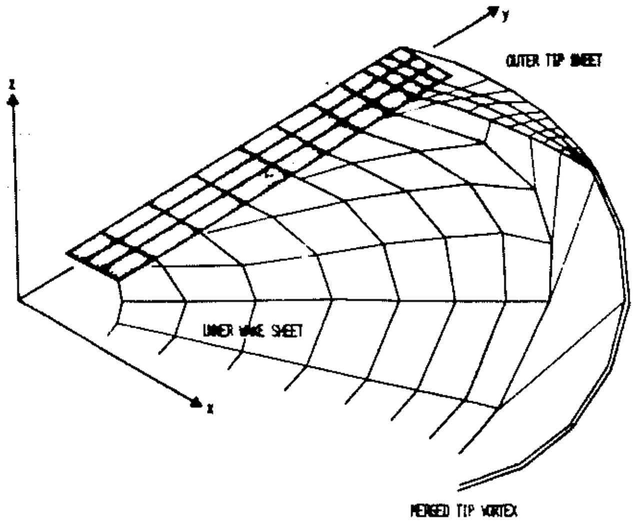

Fig. 1. Rotor Blade Vortex-Lattice Model.

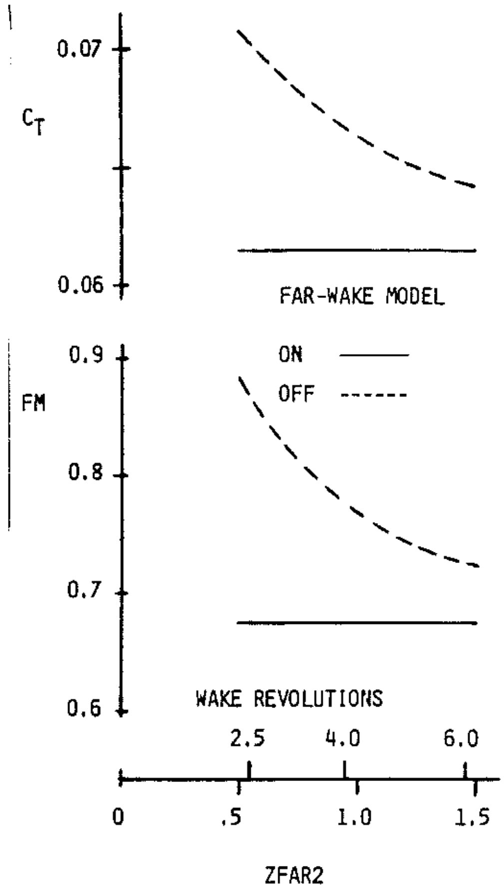

Fig. 3. Thrust and Figure of Merit Dependency on Wake Length for a Two-Bladed Rotor

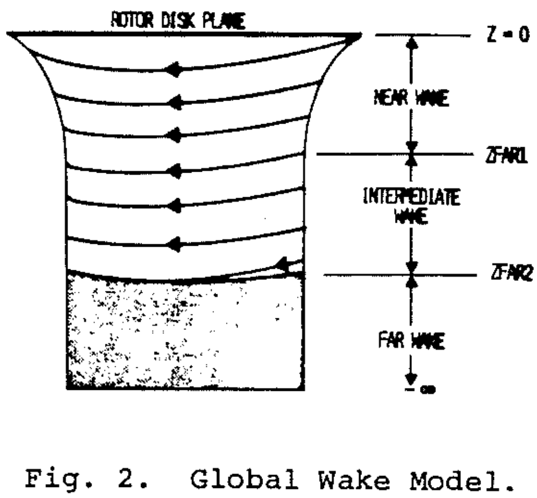

Fig. 2. Global Wake Model.

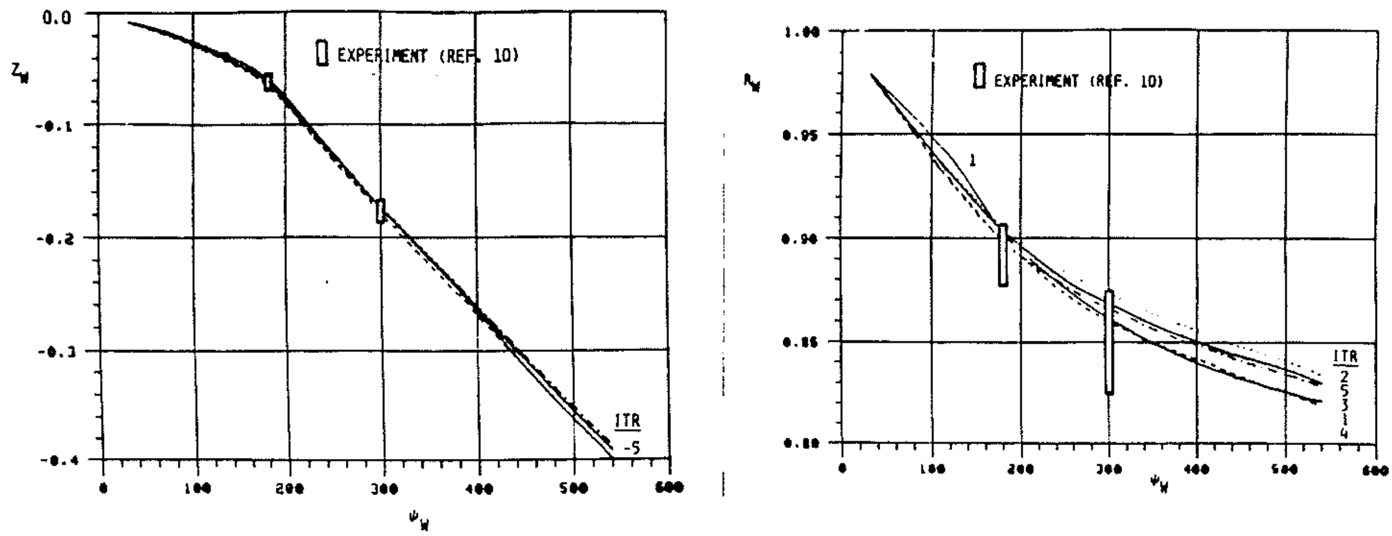

(a) Axial Coordinates.　　　(b) Radial Coordinates.

Fig. 4. Comparison of Experimental and Calculated Tip-Vortex Geometry for the Untwisted Rotor of Reference 10.

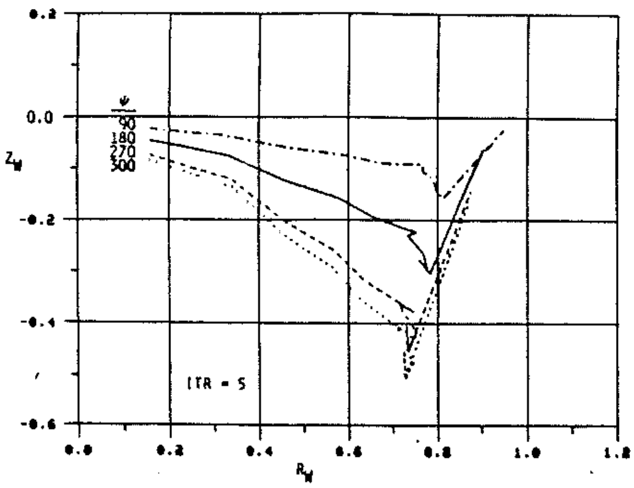

Fig. 5. Final Calculated Relaxed Wake Geometry at Constant Azimuth for the Untwisted Rotor of Reference 10.

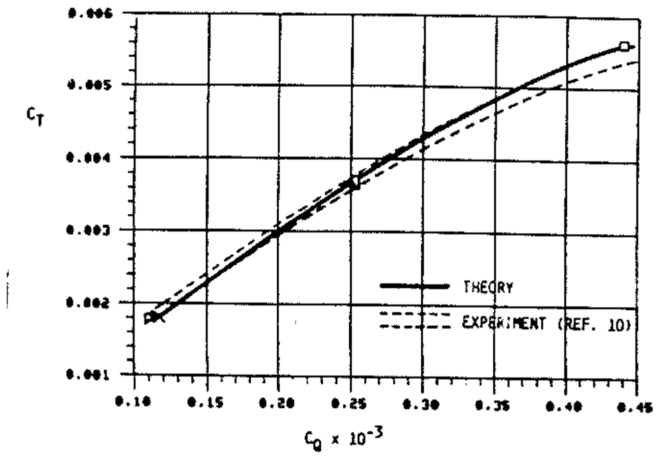

Fig. 6. Comparison of Calculated and Experimental Hover Performance for the Untwisted Rotor of Reference 10.

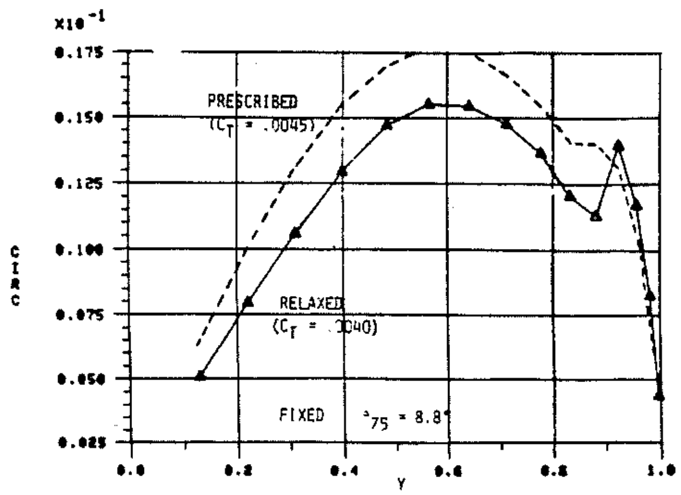

Fig. 7. Comparison of the Prescribed and Final Relaxed Wake Circulation Distribution for the Bingham Rotor at Fixed Collective (θ_{75} = 8.8°).

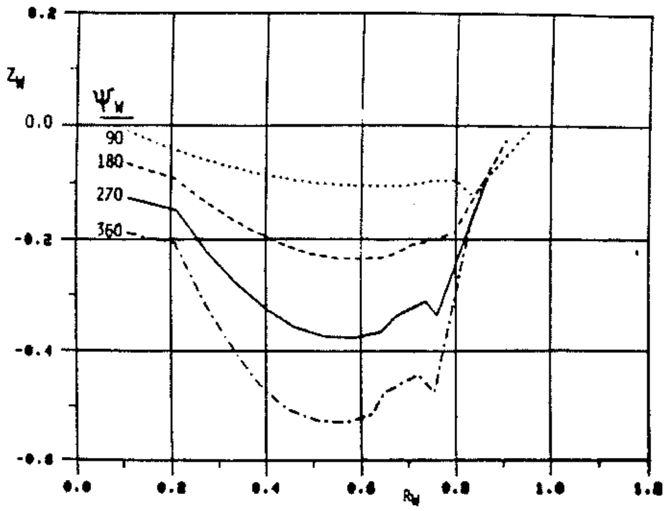

Fig. 8. Final Calculated Relaxed Wake Geometry at Constant Azimuth for the Bingham Rotor (θ_{75} = 8.8°).

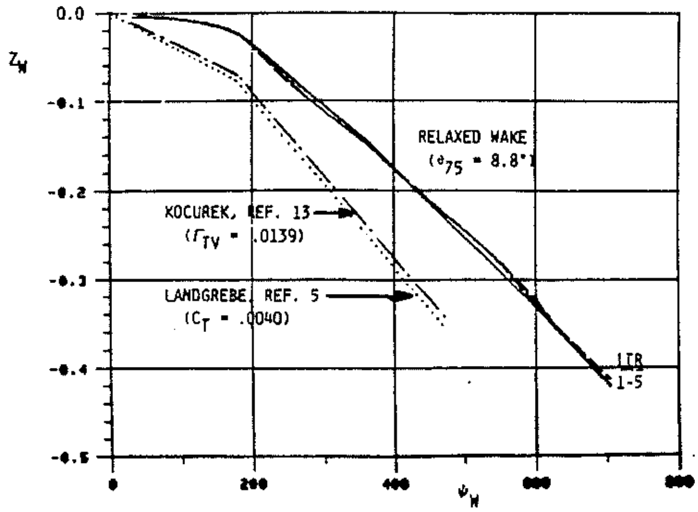

(a) Axial Coordinates.

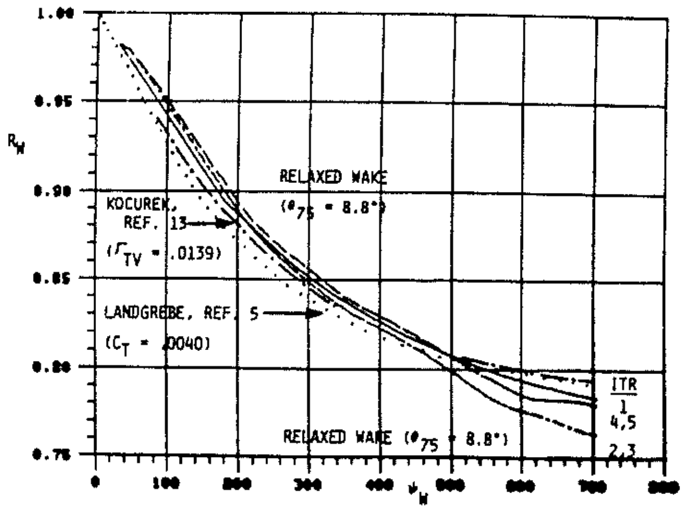

(b) Radial Coordinates.

Fig. 9. Comparison of Prescribed and Relaxed Tip-Vortex Geometry for the Bingham Rotor.

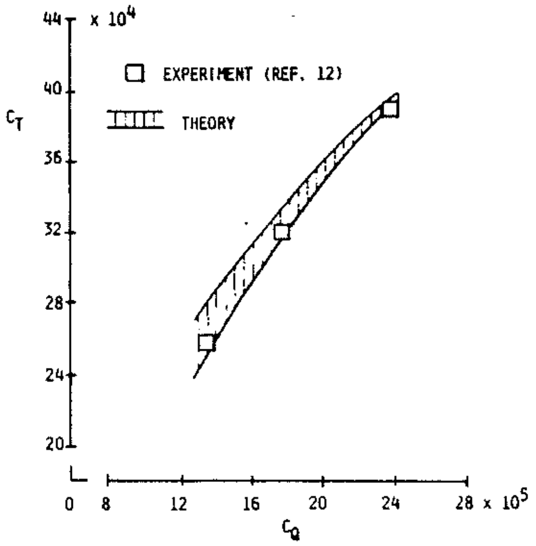

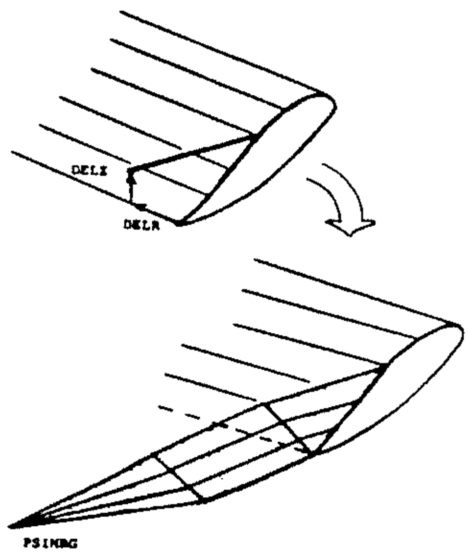

Fig. 10. Comparison of Calculated and Experimental Hover Performance for the Bingham Rotor.

Fig. 11. Rotor Tip Wake Separation (Program ROTAIR.

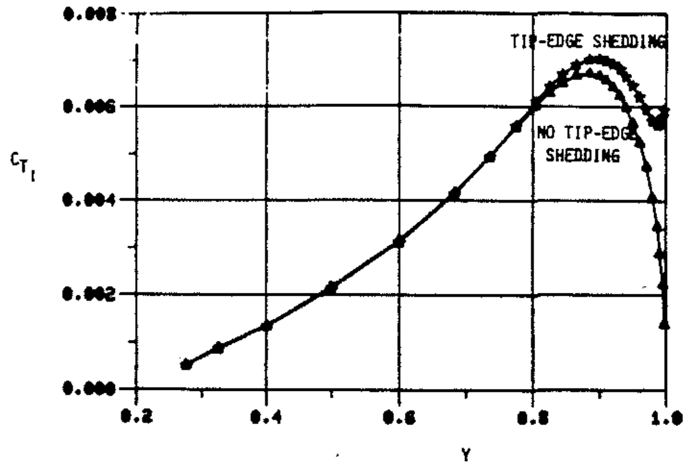

Fig. 12. Calculated Influence of Tip-Edge Vortex Shedding on Radial Thrust Loading for as Aspect Ratio 3 Rotor.

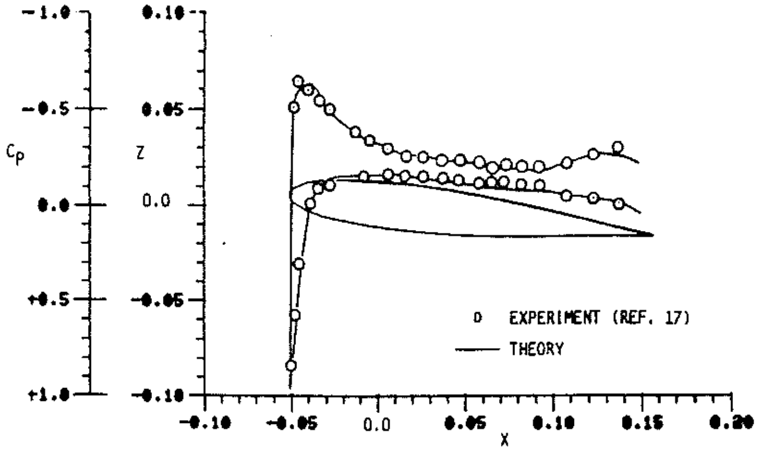

(a) Y = 0.987.

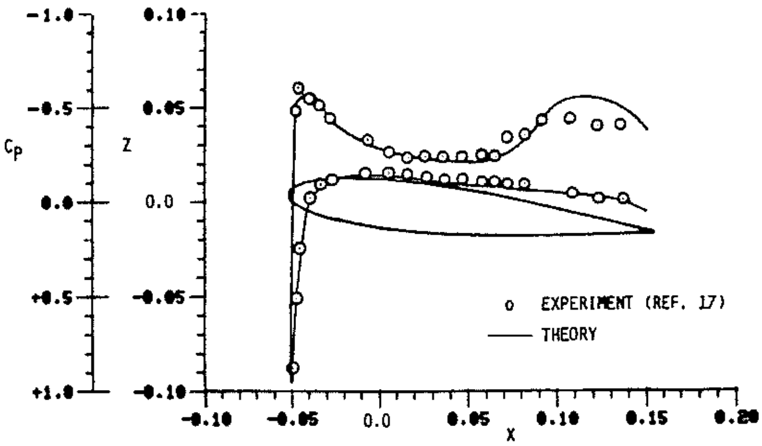

(b) Y = 0.991.

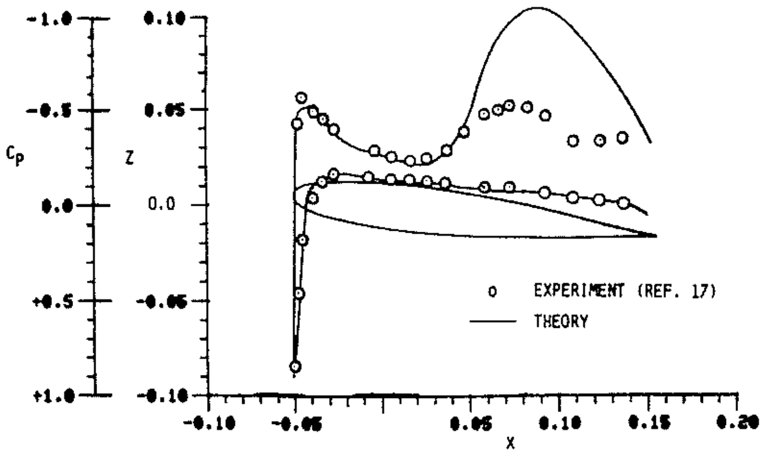

(c) Y = 0.995.

Fig. 13. Comparisons of Experimental and Calculated Chordwise Pressure Distributions for an Aspect Ratio 3 Rotor (DELZ = 0.01, DELR = 0.15, θ_{75} = 6.2°).